

The petroclinoid ligament: a meta-analysis of its morphometry and prevalence of mineralization with a review of the literature

D. Plutecki¹, P. Ostrowski², M. Bonczar², J. Iwanaga³, J. Walocha², A. Pękala², E. Szczepanek², R.S. Tubbs³, M. Loukas⁴, G. Wysiadecki⁵, M. Koziej²

¹Collegium Medicum, Jan Kochanowski University, Kielce, Poland

²Department of Anatomy, Jagiellonian University Medical College, Krakow, Poland

³Department of Neurosurgery, Tulane University School of Medicine, New Orleans, Louisiana, United States

⁴Department of Anatomical Sciences, St. George's University, Grenada, West Indies

⁵Department of Normal and Clinical Anatomy, Medical University of Lodz, Poland

[Received: 3 August 2022; Accepted: 9 September 2022; Early publication date: 27 September 2022]

Background: The petroclinoid ligament (PCL) is an important structure in the petroclival region. The anatomy of the PCL and its relationship with the surrounding structure is highly variable. The aim of this study was to estimate the morphometry, prevalence of mineralization, and anatomy of the PCL. To achieve this, the authors carried out a meta-analysis, including all studies that report extractable data on the PCL.

Materials and methods: Major online medical databases such as PubMed, Scopus, ScienceDirect, Web of Science, SciELO, BIOSIS, Current Content Connect, Korean Journal Database, and Russian Citation Index were searched to gather all studies regarding the anatomical characteristics, morphometry, and relationship with the anatomical surroundings of the PCL.

Results: A total of 25 studies were included in this meta-analysis. Data were gathered and analysed in eight categories: (1) mineralization of the PCL, (2) relationship of the abducens nerve with the PCL, (3) relationship of the dorsal meningeal artery with the PCL, (4) shape, number, and continuity of the PCL, (5) PCL anterior attachment, (6) PCL anterior attachment point on bone, (7) PCL posterior attachment point on bone, (8) morphometric features of the PCL.

Conclusions: In conclusion, the authors of the present study believe that this is the most accurate and up-to-date meta-analysis regarding the morphology and mineralization of the PCL. The data provided by the present study may be a useful tool for surgeons performing neurosurgical procedures, such as endoscopic transnasal surgeries. Detailed anatomical knowledge of the petroclival region can surely prevent surgical complications when operating in this area. (Folia Morphol 2023; 82, 3: 487–497)

Key words: petroclinoid ligament, Gruber ligament, petroclival region, mineralization, neurosurgery

Address for correspondence: Dr. M. Koziej, Department of Anatomy, Jagiellonian University Medical College, ul. Mikołaja Kopernika 12, 33–332 Kraków, Poland, tel: +48 888 202 628, e-mail: mateusz.koziej@gmail.com

This article is available in open access under Creative Common Attribution-Non-Commercial-No Derivatives 4.0 International (CC BY-NC-ND 4.0) license, allowing to download articles and share them with others as long as they credit the authors and the publisher, but without permission to change them in any way or use them commercially.

INTRODUCTION

The petroclinoid ligament (PCL), also called the petrosphenoidal ligament (PSL), or Gruber's ligament (GL), is a fibrous structure in the petroclival region. It was first described in 1859 by Wenzel Leopold Gruber, a Russian physician and anatomist [7]. The PCL is usually described as a butterfly- or triangular-shaped structure that extends from the petrous tubercle of the petrous apex posteriorly and attaches to the posterior clinoid process anteriorly [1]. The PCL forms the superior portion of the Dorello canal (DC), which contains the abducens nerve (AN), the inferior petrosal sinus, and the dorsal meningeal artery (DMA) [29]. PCL and its close anatomical area are presented on Figures 1 and 2.

Ossification of the PCL have been described in the literature. The cause of ossification is usually said to be age-related. However, it has also been presented as a radiographic characteristic of basal cell carcinoma syndrome and systemic fluorosis [2]. Mineralization of ligaments can cause complications in surgical access, alter the appearance of important anatomical landmarks, or prevent mobilization of important structures during surgery [28].

Understanding the variability in the morphology and ossification of the PCL can be of great clinical significance when performing neurosurgical procedures in the petroclival region, such as endoscopic transnasal surgeries. The PCL has also been described as a useful landmark to locate the AN in tumour removal surgeries using the transnasal approach [27]. Therefore, the objective of the present study was to provide useful data on the morphometry, prevalence of calcifications, and anatomy of the PCL. To achieve this, a systematic search of the literature and a meta-analysis were performed. To the best knowledge of the authors, this is the first meta-analysis regarding the morphology and ossification of the PCL.

MATERIALS AND METHODS

Search strategy

Major online medical databases such as PubMed, Scopus, ScienceDirect, Web of Science, SciELO, BIOSIS, Current Content Connect, Korean Journal Database, and Russian Citation Index were searched to gather all studies on anatomical characteristics, morphometry, and relationships with surrounding structures of the PCL. The study collection ended in April 2022. In agreement with the Boolean technique, the following search terms were employed: (petroclinoid ligament)

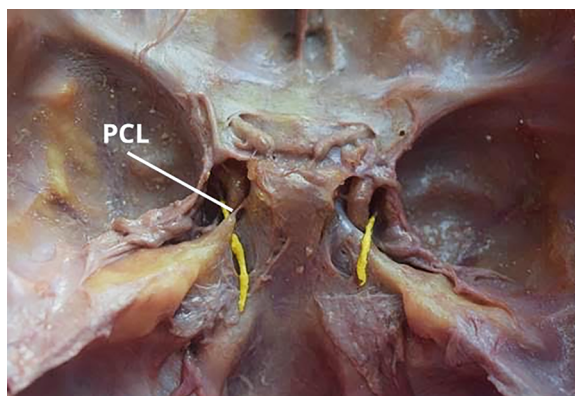


Figure 1. Petroclinoid ligament (PCL) and its close anatomical area.

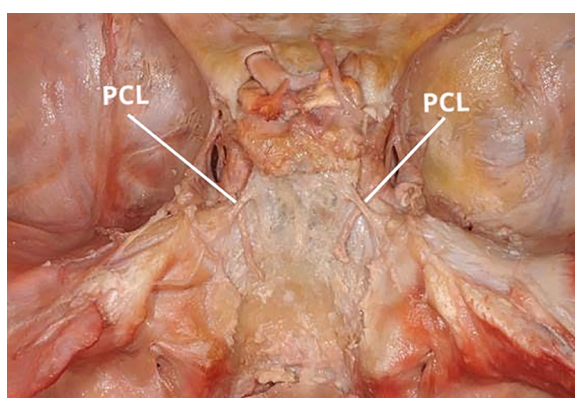


Figure 2. Petroclinoid ligament (PCL) and its close anatomical area.

OR (petroclinoid fold) OR (petrosphenoidal ligament) OR (Gruber's ligament) OR (paraclinoid region). The search terms were individually adapted to each database to minimise potential bias. Neither date, language, article type, nor text availability conditions were applied. An additional search was conducted through the references of the identified studies at the end of the search stage to ensure the accuracy of the process. During the study, the Preferred Reporting Items for Systematic Reviews and Meta-Analyses (PRISMA) guidelines were followed. Furthermore, the Critical Appraisal Tool for Anatomical Meta-analysis (CATAM) was used to provide the highest quality findings [3].

Eligibility assessment

The database search and the manual search identified a total of 518 studies that were initially evaluated by two independent reviewers. After removing duplicates and irrelevant records, a total of 145 articles were qualified for a full-text evaluation. To minimise potential bias and maintain accurate statistical meth-

odology, articles such as case reports, case series, conference reports, reviews, letters to editors, and studies that provided incomplete or irrelevant data were excluded. The inclusion criteria consisted of original studies with extractable numerical data regarding the topic of this study. Finally, a total of 25 studies were included in this meta-analysis. Additionally, the AQUA Tool which was specifically designed for anatomical meta-analyses was used to minimise the potential bias of included studies [8].

Data extraction

Data from qualified studies were extracted by two independent reviewers. Qualitative data, such as year of publication, country and continent of origin, data collection methodology and information on diseases in the studied groups, were collected. Quantitative data, such as sample size, numerical data on anatomical characteristics, morphometry, and relationship with the anatomical surroundings of the PCL were also gathered. Any discrepancies between studies, identified by the two reviewers, were resolved by contacting the authors of the original studies whenever possible or by consensus with a third reviewer.

Statistical analysis

To perform the meta-analyses, STATISTICA version 13.1 software (StatSoft Inc., Tulsa, OK, USA), MetaXL version 5.3 software (EpiGear International Pty Ltd., Wilston, Queensland, Australia), and Comprehensive Meta-analysis version 3.0 software (Biostat Inc., Englewood, NJ, USA) were used. A random-effects model was used in all analyses. The heterogeneity among the studies was evaluated, using both the Chi-squared test and the I-squared statistic [9]. The I-squared statistic was interpreted as follows: 0–40% as “might not be important”; 30–60% as “may represent moderate heterogeneity”; 50–90% as “may represent substantial heterogeneity”; 75–100% as “may represent considerable heterogeneity”. P-value of < 0.05 and the confidence intervals (95% CI) were used to find statistically significant differences between the studied groups. In the case of overlapping confidence intervals, differences were considered statistically insignificant.

RESULTS

Search results

After the selection of the initially accepted 77 studies, a total of 52 studies were excluded. Most of

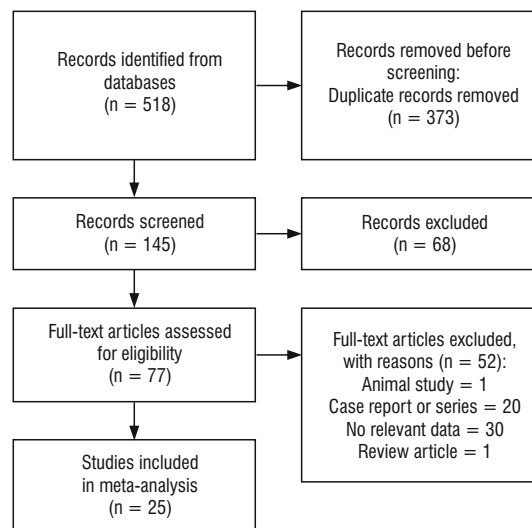


Figure 3. Flow diagram presenting process of collecting data included in this meta-analysis

them ($n = 30$) were disqualified due to the lack of relevant data. Twenty case reports from case series were excluded. Furthermore, two studies were excluded because they were a review article and an animal study. Eventually, a total of 25 studies were included in this meta-analysis [1, 2, 4–6, 10–16, 19–28, 32–34]. According to the PRISMA guidelines, an overall data collection process is presented in Figure 3. Additionally, the characteristics of all the submitted studies are collected in Table 1.

Mineralization of the PCL

A total of 5592 ligaments were analysed in relation to their mineralization process. Seven categories of data were established from the submitted studies: (1) subgroup in which the PCL mineralization process was not observed; (2) subgroup in which the PCL mineralization process was not observed; (3) subgroup in which complete mineralization of the PCL was observed; (4) subgroup of data collected from the studies in which the authors did not specify the degree of mineralization; however, any progress of mineralization was observed; (5) subgroup of patients in whom the mineralization process was observed bilaterally; (6) subgroup of patients in whom the mineralization process was observed unilaterally; (7) subgroup of patients in whom the other mineralization of head ligaments were observed. The pooled prevalence of any mineralization process was established to be 10.06% (95% CI: 5.61–15.27%). Despite the general results, additional regional and

Table 1. Characteristics of studies included in this meta-analysis

First author [reference]	Year	Region	Country	Type of study	Type of examination	Thickness slice [mm]
Ghorbanlou et al. [6]	2022	Asia	Iran	Radiological	CT	0.675
Kayaci et al. [14]	2021	Asia	Turkey	Cadaveric	–	–
Wysiadecki et al. [34]	2021	Europe	Poland	Cadaveric	–	–
Iwanaga et al. [13]	2020	North America	USA	Cadaveric	–	–
Touska et al. [28]	2019	Europe	UK	Radiological	CT	0.6
Bayrak et al. [1]	2019	Asia	Turkey	Radiological	CT	0.3
Kumar et al. [15]	2018	Asia	India	Cadaveric	–	–
Ozdede et al. [19]	2018	Asia	Turkey	Radiological	CT	0.4
Inal et al. [12]	2016	Asia	Turkey	Radiological	CT	0.67
Özgür and Esen [21]	2015	Asia	Turkey	Radiological	CT	0.5
Tomio et al. [27]	2015	Asia	Indonesia	Cadaveric	–	–
Wysiadecki et al. [33]	2015	Europe	Poland	Cadaveric	–	–
Ezer et al. [5]	2012	North America	USA	Cadaveric	–	–
Sedghizadeh et al. [24]	2012	North America	USA	Radiological	CT	–
Icke et al. [11]	2010	Asia	Turkey	Cadaveric	–	–
Ozer et al. [20]	2010	Asia	Turkey	Cadaveric	–	–
Liu et al. [16]	2009	Asia	China	Cadaveric	–	–
Skrzat et al. [25]	2007	Europe	Poland	Cadaveric	–	–
Cederberg et al. [2]	2003	North America	USA	Radiological	RTG	–
Iaconetta et al. [10]	2003	Europe	Germany	Cadaveric	–	–
Ozveren et al. [22]	2003	Asia	Turkey	Cadaveric	–	–
Destriex et al. [4]	1997	Europe	France	Cadaveric	–	–
Umansky et al. [32]	1991	Asia	Israel	Cadaveric	–	–
Rzyski and Kosowicz [23]	1975	Europe	Poland	Radiological	RTG	–
Stanton and Wilkinson [26]	1949	Europe	UK	Radiological	RTG	–

CT — computed tomography; RTG — radiograph

methodological analyses were also enrolled. All the results mentioned above and the more detailed results are gathered in Table 2.

Relationship of the abducens nerve with the PCL

An analysis of the relationship between the PCL and the AN was established considering a total of 469 ligaments. The pooled prevalence for AN to run through the PCL was enrolled as 4.95% (95% CI: 0.00–17.03%). Despite the general results, additional regional analyses were also enrolled. All the results mentioned above and the more detailed results are gathered in Table 3.

Relationship of the dorsal meningeal artery with the PCL

The analysis of the relationship between the PCL and the DMA was established considering a total of

103 ligaments. A pooled prevalence for DMA to run below PCL was enrolled as 94.40% (95% CI: 83.15–100.00%). Despite the general results, additional regional analysis was also included. All the results mentioned above and the more detailed results are gathered in Table 4.

Shape, number, and continuity of the PCL

The analyses of shapes, number, and continuity of the PCL were performed on a total of 143 ligaments. Butterfly-shaped PCL was found to be the most common, with a prevalence of 79.59% (95% CI: 21.32–100.00%). A single PCL occurs much more frequently than a double one, with a prevalence of 93.09% (95% CI: 75.50–100.00%). Despite the general results, additional regional analysis was also included. All the results mentioned above and the more detailed results are gathered in Table 5.

Table 2. Statistical results of this meta-analysis regarding the mineralization of petroclinoid ligament in each category

Category	N	Pooled prevalence	LCI	HCI	Q	I ²
Overall results	5592					
No mineralization		88.55%	80.16%	94.95%	1268.42	98.50
Partial mineralization		1.78%	0.23%	4.44%	520.65	96.35
Complete mineralization		2.20%	0.67%	4.49%	354.54	94.64
Any mineralization		10.06%	5.81%	15.27%	565.16	96.64
Bilateral		0.54%	0.10%	1.26%	113.22	83.22
Unilateral		0.75%	0.12%	1.80%	177.27	89.28
Other mineralizations of head ligaments		1.02%	0.03%	2.95%	412.96	95.40
Results gathered using radiological methods	5043					
No mineralization		78.58%	63.56%	90.63%	1171.33	99.23
Partial mineralization		3.07%	0.26%	8.06%	497.83	98.19
Complete mineralization		2.86%	0.52%	6.66%	335.77	97.32
Any mineralization		17.06%	9.69%	25.92%	504.64	98.22
Bilateral		0.44%	0.00%	1.43%	108.72	91.72
Unilateral		0.51%	0.00%	1.58%	167.25	94.62
Other mineralizations of head ligaments		1.61%	0.00%	4.48%	407.71	97.79
Results gathered from cadavers	549					
No mineralization		96.75%	94.37%	98.53%	14.13	36.31
Partial mineralization		0.55%	0.07%	1.38%	0.73	0.00
Complete mineralization		1.03%	0.23%	2.28%	10.78	16.49
Any mineralization		3.25%	1.47%	5.63%	14.13	36.31
Bilateral		0.40%	0.02%	1.15%	3.94	0.00
Unilateral		1.28%	0.48%	2.42%	7.10	0.00
Other mineralizations of head ligaments		0.57%	0.08%	1.42%	4.24	0.00
Results gathered in Asia	2681					
No mineralization		91.98%	85.59%	96.70%	188.14	95.22
Partial mineralization		1.13%	0.00%	3.14%	117.54	92.34
Complete mineralization		2.84%	0.00%	8.90%	304.29	97.04
Any mineralization		1.07%	0.05%	3.04%	79.56	88.69
Bilateral		0.30%	0.00%	0.93%	25.37	64.52
Unilateral		0.60%	0.00%	1.63%	55.29	83.72
Other mineralizations of head ligaments		0.20%	0.02%	0.53%	13.14	31.50
Results gathered in Europe	1623					
No mineralization		81.80%	55.28%	100.00%	678.82	99.12
Partial mineralization		2.36%	0.00%	7.05%	81.50	92.64
Complete mineralization		0.95%	0.35%	1.81%	9.10	34.04
Any mineralization		11.56%	2.83%	24.32%	194.88	96.92
Bilateral		0.84%	0.00%	3.29%	75.79	92.08
Unilateral		1.41%	0.00%	4.68%	89.35	93.28
Other mineralizations of head ligaments		1.11%	0.00%	3.36%	35.85	83.26
Results gathered in North America	1288					
No mineralization		88.14%	61.15%	100.00%	156.44	98.72
Partial mineralization		4.15%	0.00%	27.12%	197.06	98.99
Complete mineralization		3.46%	0.24%	9.23%	17.19	88.36
Any mineralization		11.86%	0.00%	38.85%	156.44	98.72
Bilateral		0.67%	0.00%	2.08%	6.54	69.40
Unilateral		0.39%	0.00%	1.76%	8.64	76.85
Other mineralizations of head ligaments		5.57%	0.00%	38.24%	285.69	99.30

LCI — lower confidence interval; HCI — higher confidence interval; Q — Cochran's Q

PCL general anterior attachment

An analysis of anterior PCL attachment was performed on a total of 330 ligaments. The studies included in this meta-analysis were not precise with regard to attachment. Therefore, the authors estab-

lished four subcategories of data: (1) PCL attaches to a bone; (2) PCL attaches to the dura mater; (3) PCL attaches to a bone and the dura mater; and (4) PCL attached to a bone and a second bone. The most frequent anterior attachment was found to be PCL

Table 3. Statistical results of this meta-analysis regarding the relationship of the abducens nerve (AN) to the petroclinoid ligament (PCL) in each category

Category	N	Pooled prevalence	LCI	HCI	Q	I ²
Overall results	469					
AN runs below the PCL		93.02%	79.67%	100.00%	288.75	95.50
AN runs above the PCL		1.57%	0.62%	2.92%	10.29	0.00
AN runs through the PCL		4.95%	0.00%	17.03%	300.24	95.67
Results gathered in Asia	274					
AN runs below the PCL		88.03%	55.49%	100.00%	270.68	97.41
AN runs above the PCL		1.16%	0.15%	2.90%	7.22	3.01
AN runs through the PCL		10.06%	0.00%	41.56%	277.49	97.48
Results gathered in Europe	152					
AN runs below the PCL		97.61%	94.46%	99.55%	1.79	0.00
AN runs above the PCL		2.39%	0.45%	5.54%	1.79	0.00
AN runs through the PCL		0.00%	0.00%	0.00%	0.00	0.00
Results gathered in North America	43					
AN runs below the PCL		98.96%	94.83%	100.00%	0.14	0.00
AN runs above the PCL		0.00%	0.00%	0.00%	0.00	0.00
AN runs through the PCL		0.00%	0.00%	0.00%	0.00	0.00

LCI — lower confidence interval; HCI — higher confidence interval; Q — Cochran's Q

Table 4. Statistical results of this meta-analysis regarding the relationship of the dorsal meningeal artery (DMA) to the petroclinoid ligament (PCL) in each category

Category	N	Pooled prevalence	LCI	HCI	Q	I ²
Overall results	103					
DMA runs below the PCL		94.40%	83.15%	100.00%	8.71	65.56
DMA runs above the PCL		3.01%	0.00%	9.59%	7.33	59.06
Results gathered in Asia	30					
DMA runs below the PCL		90.80%	72.67%	100.00%	1.97	49.30
DMA runs above the PCL		9.20%	0.00%	27.33%	1.97	49.30

LCI — lower confidence interval; HCI — higher confidence interval; Q — Cochran's Q

attachment to the bone with a prevalence of 94.43% (95% CI: 85.60–100.00%). Despite the general results, additional regional analysis was also included. All the results mentioned above and the more detailed results are gathered in Table 6.

PCL anterior attachment point on the bone

Analysis of the anterior attachment point of the PCL on the bone was carried out in a total of 297 ligaments. The most common anterior attachment point was found to be in the posterior clinoid process with a prevalence of 72.95% (95% CI: 28.05–100.00%). Despite the general results, additional regional analysis was also included. All the results mentioned above and the more detailed results are gathered in Table 7.

PCL posterior attachment point on the bone

Analysis of the posterior attachment point of the PCL on the bone was carried out in a total of 297 ligaments. The most common posterior attachment point was found to be in the petrous apex with a prevalence of 86.00% (95% CI: 55.13–100.00%). Despite the general results, additional regional analysis was also included. All the results mentioned above and the more detailed results are gathered in Table 8.

Morphometric features of the PCL

From the submitted studies, a total of eight categories were established regarding the morphological characteristics of the PCL: (1) length; (2) left PCL length; (3) right PCL length; (4) width; (5) thickness;

Table 5. Statistical results of meta-analysis regarding the anatomical features, like shape, number and continuity of the petroclinoid ligament (PCL) in each category

Category	N	Pooled prevalence	LCI	HCI	Q	I ²
Overall results	143					
Butterfly-shaped PCL		79.59%	21.32%	100.00%	175.71	97.72
Y-shaped PCL		4.12%	0.00%	14.95%	25.82	84.51
Triangular PCL		3.60%	0.00%	12.32%	19.63	79.63
Single PCL		93.09%	75.50%	100.00%	42.19	90.52
Double PCL		5.03%	1.03%	11.32%	7.12	43.85
Complete PCL		6.19%	0.00%	27.49%	60.03	93.34
Incomplete PCL		4.86%	0.00%	19.46%	37.88	89.44
Hypoplastic/Fragmented	5592	0.66%	0.16%	1.44%	113.55	83.27
Results gathered in Asia	70					
Butterfly-shaped PCL		92.90%	74.28%	100.00%	10.06	80.12
Y-shaped PCL		0.97%	0.00%	3.91%	0.20	0.00
Triangular PCL		7.10%	0.00%	25.72%	10.06	80.12
Single PCL		97.96%	94.02%	100.00%	1.94	0.00
Double PCL		7.61%	2.38%	15.12%	1.19	0.00
Complete PCL		12.81%	0.00%	61.07%	33.03	93.94
Incomplete PCL		9.84%	0.00%	42.39%	20.35	90.17
Hypoplastic/Fragmented	2681	8.02%	3.30%	14.41%	188.14	95.22

LCI — lower confidence interval; HCI — higher confidence interval; Q — Cochran's Q

Table 6. Statistical results of this meta-analysis regarding the anterior attachment of the petroclinoid ligament (PCL) in each category

Category	N	Pooled prevalence	LCI	HCI	Q	I ²
General results	330					
PCL attaches to a bone		94.43%	85.60%	100.00%	76.79	88.28
PCL attaches to the dura mater		2.88%	0.55%	6.63%	20.43	55.95
PCL attaches to a bone and the dura mater		2.32%	0.00%	6.39%	36.10	75.07
PCL attaches to a bone and a bone		0.86%	0.10%	2.21%	5.45	0.00
Results gathered in Asia	219					
PCL attaches to a bone		99.24%	97.89%	100.00%	4.10	0.00
PCL attaches to the dura mater		0.76%	0.00%	2.11%	4.10	0.00
PCL attaches to a bone and the dura mater		0.00%	0.00%	0.00%	0.00	0.00
PCL attaches to a bone and a bone		0.00%	0.00%	0.00%	0.00	0.00
Results gathered in Europe	68					
PCL attaches to a bone		92.34%	84.65%	97.66%	0.82	0.00
PCL attaches to the dura mater		7.66%	2.34%	15.35%	0.82	0.00
PCL attaches to a bone and the dura mater		0.00%	0.00%	0.00%	0.00	0.00
PCL attaches to a bone and a bone		0.00%	0.00%	0.00%	0.00	0.00
Results gathered in North America	43					
PCL attaches to a bone		75.50%	0.00%	100.00%	15.94	93.73
PCL attaches to the dura mater		7.09%	0.00%	21.99%	1.53	34.62
PCL attaches to a bone and the dura mater		15.48%	0.00%	59.04%	6.99	85.69
PCL attaches to a bone and a bone		4.91%	0.16%	13.83%	0.46	0.00

LCI — lower confidence interval; HCI — higher confidence interval; Q — Cochran's Q

Table 7. Statistical results of this meta-analysis regarding the anterior attachment point of the petroclinoid ligament (PCL) on the bone in each category

Category	N	Pooled prevalence	LCI	HCI	Q	I ²
Overall results	297					
On clivus		58.25%	7.68%	100.00%	528.14	98.49
Under posterior clinoid process		72.95%	28.05%	100.00%	426.46	98.12
On dorsum sellae		27.05%	0.00%	71.95%	426.46	98.12
Results gathered in Asia	219					
On clivus		52.44%	0.00%	100.00%	344.25	98.55
Under posterior clinoid process		90.01%	59.42%	100.00%	143.95	96.53
On dorsum sellae		25.10%	0.00%	72.15%	202.81	97.53
Results gathered in Europe	68					
On clivus		49.16%	0.00%	100.00%	130.96	99.24
Under posterior clinoid process		49.16%	0.00%	100.00%	130.96	99.24
On dorsum sellae		50.84%	0.00%	100.00%	130.96	99.24

LCI — lower confidence interval; HCI — higher confidence interval; Q — Cochran's Q

Table 8. Statistical results of this meta-analysis regarding the posterior attachment point of the petroclinoid ligament (PCL) on the bone in each category

Category	N	Pooled prevalence	LCI	HCI	Q	I ²
Overall results	297					
On petrous apex		86.00%	55.13%	100.00%	291.71	97.26
On petrous ridge		4.75%	0.00%	14.07%	73.47	89.11
On petrous tubercle		6.07%	0.00%	27.10%	237.82	96.64
Results gathered in Asia	219					
On petrous apex		99.41%	98.20%	100.00%	0.74	0.00
On petrous ridge		0.00%	0.00%	0.00%	0.00	0.00
On petrous tubercle		0.00%	0.00%	0.00%	0.00	0.00
Results gathered in Europe	68					
On petrous apex		54.71%	0.00%	100.00%	110.94	99.10
On petrous ridge		0.71%	0.00%	3.41%	0.02	0.00
On petrous tubercle		45.29%	0.00%	100.00%	110.94	99.10

LCI — lower confidence interval; HCI — higher confidence interval; Q — Cochran's Q

(6) medial insertion; (7) lateral insertion and (8) mid-point. The results for each category are summarized in Table 9.

DISCUSSION

The morphology and variations of the PCL have been discussed extensively in the literature. The structure of the PCL has been described as being either butterfly- or triangular-shaped. Icke et al. [11] reported that 78% of PCLs were butterfly-shaped and 22% triangular. Iwanaga et al. [13] presented variations in PCL morphology in a study consisting of 36 sides of 18 fresh-frozen adult cadaveric heads. In the study, the shape of the PCL was described differently than that

of a butterfly or a triangular shape. The PCL was categorized into three groups, which were, single-band type, Y-shaped type, and duplicated type. The single-band type was the most frequently observed type (58.1%). However, the results of the present meta-analysis show that the butterfly-shaped PCL is the most frequent type (79.59%).

There has been a lot of controversy with respect to the PCL attachment points, more specifically its anterior attachment point. The PCL was previously described as a ligament that extends from the posterior clinoid process anteriorly to its posterior attachment at the petrous tubercle of the petrous apex [11, 35]. However, a recent cadaveric study conducted

Table 9. Statistical result of meta-analysis regarding morphometrical features of petroclinoid ligament (PCL) in each category

Category	Mean	Standard error	Variance	Lower limit	Upper limit	Z-value	P-value
Length	11.05	1.00	1.00	9.09	13.01	11.06	0.00
Left PCL length	8.03	1.43	2.05	5.23	10.84	5.61	0.00
Right PCL length	8.01	1.53	2.34	5.01	11.01	5.24	0.00
Width	2.64	0.48	0.23	1.70	3.58	5.51	0.00
Thickness	0.74	0.22	0.05	0.31	1.18	3.34	0.00
Medial insertion	4.39	0.31	0.09	3.79	5.00	14.25	0.00
Lateral insertion	4.95	0.55	0.30	3.87	6.03	9.00	0.00
Midpoint	2.40	0.35	0.12	1.71	3.08	6.85	0.00

by Iwanaga et al. [13] states otherwise. In the study, the anterior attachment of the PCL was divided into two categories; PCL with an anterior attachment to the dura mater, or PCL with an anterior attachment to bone. When the PCL had an attachment to bone, the point of attachment was the lateral aspect of the upper clivus rather than the posterior clinoid process. However, the posterior attachment of the PCL was always at the petrous apex. Therefore, the authors of that study stated that the PCL should be described as the petroclival ligament because it represents this structure better and more accurately. The results of the present meta-analysis show that the most common anterior attachment of the PCL is the posterior clinoid process (72.95%), and the most frequently reported posterior attachment is the petrous apex (86.00%). Therefore, a change in the nomenclature of the PCL seems redundant.

The PCL forms the superior part of the DC. The DC was first described by Gruber in 1859 [7], as an osteofibrous canal at the apex of the petrous bone, containing the abducens nerve and the inferior petrosal sinus. Since then, numerous studies have been published on the morphology and clinical significance of DC. The AN has been described as a constant structure in the DC, with some studies reporting the nerve in 100% of the specimens [30, 32]. However, the present study shows that the prevalence of the AN going under the PCL (meaning inside the DC) is 93.02%. Tubbs et al. [30] presented an anatomical study on the DC and abducens nerve. In the study, a secondary tunnel was found within the DC that exclusively contained the abducens nerve. This structure limited the mobility of the AN, making it more susceptible to head trauma-induced injury. The DC also contains the DMA, which is said to supply the petroclival portion of the AN and the superior clival

dura, among others [17]. The data of this meta-analysis show that the DMA should be considered as a quite constant structure of the DC, with a prevalence of 94.40%.

The literature has been ambiguous regarding the nomenclature of the PCL. As mentioned above, some authors have used different terms when dealing with this structure. The other terms used for PCL include the Gruber ligament, the petrosphenoidal ligament, and the petroclival ligament [13]. Furthermore, it is crucial to understand that the PCL and posterior petroclinoid fold are two independent structures. The petroclinoid fold is a fold of the dura mater that extends between the anterior and posterior clinoid processes and the petrosal part of the temporal bone, and should not be referred to as a ligament [34]. Based on the results of the present meta-analysis, the PCL should be referred to as the petroclinoid ligament, because it represents this structure in the most precise way.

The PCL can undergo ossification causing changes in the anatomy of the base of the skull. The degree of ossification of PCL varies from being only partially ossified to being completely ossified, forming a bony bridge. Ossification can be unilateral or bilateral. The results of this meta-analysis show that the prevalence of ossification of PCL unilaterally is slightly higher (0.75%) than bilaterally (0.54%). Interestingly, the prevalence of complete PCL ossification was significantly higher in North America (3.46%) than in Europe (0.95%), even though the number of specimens in North America was lower by 335 PCLs. Although PCL ossification is said to be age-related, some studies have reported that it may also be a radiographic feature of basal cell carcinoma syndrome and systemic fluorosis [2].

Petroclinoid ligament ossification can increase the risk of AN injury. Tubbs et al. [31] reported that clini-

cians should consider ossification of PCL in patients with unexplained cases of AN palsy. In a radiological study conducted by Inal et al. [12] the calcification at the petroclival region was investigated using multiple slice computed tomography of the skull base. In the study, the clinical significance of PCL ossification was described. It was stated that if the PCL was ossified in patients with increased intracranial pressure syndrome, the pressure would not affect the AN passing under the PCL because the ligament would be hard and protect the nerve superiorly. Therefore, AN palsy would develop slower. On the contrary, the oculomotor nerve is superior to the PCL and DC. In the cases where PCL is ossified and lateral transtentorial herniation occurs, oculomotor nerve palsy would develop more rapidly.

Knowledge about the morphology of the PCL could be of great importance in neurosurgical procedures. Endoscopic transnasal surgeries are a good alternative for the treatment of skull base lesions. Tomio et al. [27] performed a cadaveric study in which they described the PCL as the most reliable landmark of the AN in the transnasal transclival view. They concluded that the PCL was a useful structure for locating the AN in tumour removal surgeries that use this approach. The PCL is also of significant clinical importance due to its proximity to the oculomotor nerve. During head trauma, downward displacement of the brain stem can result in damage to the pupilomotor fibres on the ventromedial surface of the oculomotor nerve, located on the PCL. This can lead to internal ophthalmoplegia [18].

Limitations of the study

This study is not without limitations and is burdened with potential bias, as the results of this meta-analysis may reflect anatomical variations of the Asian people, rather than of the global population. A potential sexual dimorphism in the anatomical features of the PCL was not established due to the lack of data. Analogically, no gender-related statistics were enrolled. Moreover, an analysis of morphometrical features of the PCL was not enrolled in relation to height of the subjects nor any other parameters due to lack of such information in primary studies.

CONCLUSIONS

In conclusion, the authors of the present study believe that this is the most accurate and up-to-date meta-analysis regarding the morphology and miner-

alization of the PCL. The most common attachment points of the PCL were the posterior clinoid process anteriorly (72.95%), and the petrous apex posteriorly (86.00%). The AN was most commonly found under the PCL, in the DC (93.02%), however, variations of the course of the AN fibres might occur. The data provided by the present study may be a useful tool for surgeons performing neurosurgical procedures, such as endoscopic transnasal surgeries. Detailed anatomical knowledge of the petroclival region can surely prevent surgical complications when operating in this area.

Conflict of interest: None declared

REFERENCES

1. Bayrak S, Göller Bulut D, Kurşun Çakmak EŞ, et al. Cone beam computed tomographic evaluation of intracranial physiologic calcifications. *J Craniofac Surg.* 2019; 30(2): 510–513, doi: [10.1097/SCS.0000000000004918](https://doi.org/10.1097/SCS.0000000000004918), indexed in Pubmed: [30507878](https://pubmed.ncbi.nlm.nih.gov/30507878/).
2. Cederberg RA, Benson BW, Nunn M, et al. Calcification of the interclinoid and petroclinoid ligaments of sella turcica: a radiographic study of the prevalence. *Orthod Craniofac Res.* 2003; 6(4): 227–232, doi: [10.1034/j.1600-0544.2003.00243.x](https://doi.org/10.1034/j.1600-0544.2003.00243.x), indexed in Pubmed: [14606526](https://pubmed.ncbi.nlm.nih.gov/14606526/).
3. D'Antoni AV, Tubbs RS, Patti AC, et al. The critical appraisal tool for anatomical meta-analysis: a framework for critically appraising anatomical meta-analyses. *Clin Anat.* 2022; 35(3): 323–331, doi: [10.1002/ca.23833](https://doi.org/10.1002/ca.23833), indexed in Pubmed: [35015336](https://pubmed.ncbi.nlm.nih.gov/35015336/).
4. Destrieux C, Velut S, Kakou MK, et al. A new concept in Dorello's canal microanatomy: the petroclival venous confluence. *J Neurosurg.* 1997; 87(1): 67–72, doi: [10.3171/jns.1997.87.1.0067](https://doi.org/10.3171/jns.1997.87.1.0067), indexed in Pubmed: [9202267](https://pubmed.ncbi.nlm.nih.gov/9202267/).
5. Ezer H, Banerjee AD, Thakur JD, et al. Dorello's canal for laymen: a lego-like presentation. *J Neurol Surg B Skull Base.* 2012; 73(3): 183–189, doi: [10.1055/s-0032-1311753](https://doi.org/10.1055/s-0032-1311753), indexed in Pubmed: [23730547](https://pubmed.ncbi.nlm.nih.gov/23730547/).
6. Ghorbanlou M, Moradi F, Mehdizadeh M. Frequency, shape, and estimated volume of intracranial physiologic calcification in different age groups investigated by brain computed tomography scan: a retrospective study. *Anat Cell Biol.* 2022; 55(1): 63–71, doi: [10.5115/acb.21.137](https://doi.org/10.5115/acb.21.137), indexed in Pubmed: [34866062](https://pubmed.ncbi.nlm.nih.gov/34866062/).
7. Gruber W. Anatomie des Keilbeins und Schläfenbeins. In: Richter HE, Winter A (eds.) Schmidt's Jahrbucher der Und Ausländischen. Gesamten Medicin, II, Anatomie und Physiologie 1859.
8. Henry BM, Tomaszewski KA, Ramakrishnan PK, et al. Development of the anatomical quality assessment (AQUA) tool for the quality assessment of anatomical studies included in meta-analyses and systematic reviews. *Clin Anat.* 2017; 30(1): 6–13, doi: [10.1002/ca.22799](https://doi.org/10.1002/ca.22799), indexed in Pubmed: [27718281](https://pubmed.ncbi.nlm.nih.gov/27718281/).
9. Higgins JPT, Thomas J, Chandler J. et al. (eds). *Cochrane Handbook for Systematic Reviews of Interventions.* Wiley 2019.

10. Iaconetta G, Fusco M, Samii M. The sphenopetroclival venous gulf: a microanatomical study. *J Neurosurg.* 2003; 99(2): 366–375, doi: [10.3171/jns.2003.99.2.0366](https://doi.org/10.3171/jns.2003.99.2.0366), indexed in Pubmed: [12924712](https://pubmed.ncbi.nlm.nih.gov/12924712/).
11. Icke C, Ozer E, Arda N. Microanatomical characteristics of the petrosphenoidal ligament of Gruber. *Turk Neurosurg.* 2010; 20(3): 323–327, doi: [10.5137/1019-5149.JTN.2921-10.0](https://doi.org/10.5137/1019-5149.JTN.2921-10.0), indexed in Pubmed: [20669104](https://pubmed.ncbi.nlm.nih.gov/20669104/).
12. Inal M, Muluk NB, Burulday V, et al. Investigation of the calcification at the petroclival region through multi-slice computed tomography of the skull base. *J Cranio-maxillofac Surg.* 2016; 44(4): 347–352, doi: [10.1016/j.jcms.2016.01.018](https://doi.org/10.1016/j.jcms.2016.01.018), indexed in Pubmed: [26922483](https://pubmed.ncbi.nlm.nih.gov/26922483/).
13. Iwanaga J, Altafulla JJ, Gutierrez S, et al. The Petroclinoid Ligament: Its Morphometrics, Relationships, Variations, and Suggestion for New Terminology. *J Neurol Surg B Skull Base.* 2020; 81(6): 603–609, doi: [10.1055/s-0039-1692699](https://doi.org/10.1055/s-0039-1692699), indexed in Pubmed: [33381363](https://pubmed.ncbi.nlm.nih.gov/33381363/).
14. Kayacı S, Ozveren MF, Bas O, et al. Effect of clival bone growth on the localization of the abducens nerve at the petroclival region: a postmortem anatomical study. *Surg Radiol Anat.* 2021; 43(6): 953–959, doi: [10.1007/s00276-021-02691-z](https://doi.org/10.1007/s00276-021-02691-z), indexed in Pubmed: [33687488](https://pubmed.ncbi.nlm.nih.gov/33687488/).
15. Kumar A, Sehgal R, Roy TS. Ossified ligaments in relation to foramina and bony landmarks of the middle cranial fossa. *J Anat Soc India.* 2018; 67(1): 55–60, doi: [10.1016/j.jasi.2018.03.001](https://doi.org/10.1016/j.jasi.2018.03.001).
16. Liu XD, Xu QW, Che XM, et al. Anatomy of the petrosphenoidal and petroclival ligaments at the petrous apex. *Clin Anat.* 2009; 22(3): 302–306, doi: [10.1002/ca.20771](https://doi.org/10.1002/ca.20771), indexed in Pubmed: [19173250](https://pubmed.ncbi.nlm.nih.gov/19173250/).
17. McCormack IG, Xu Lu, Nerva J, et al. Anatomy of the dorsal meningeal artery including its variations: application to skull base surgery and diagnostic and interventional imaging. *World Neurosurg.* 2021; 155: e41–e48, doi: [10.1016/j.wneu.2021.07.132](https://doi.org/10.1016/j.wneu.2021.07.132), indexed in Pubmed: [34365050](https://pubmed.ncbi.nlm.nih.gov/34365050/).
18. Nagaseki Y, Shimizu T, Kakizawa T, et al. Primary internal ophthalmoplegia due to head injury. *Acta Neurochir.* 1989; 97(3-4): 117–122, doi: [10.1007/BF01772821](https://doi.org/10.1007/BF01772821), indexed in Pubmed: [2718803](https://pubmed.ncbi.nlm.nih.gov/2718803/).
19. Ozdede M, Kayadugun A, Uçok O, et al. The assessment of maxillofacial soft tissue and intracranial calcifications via cone-beam computed tomography. *Curr Med Imag Rev.* 2018; 14(5): 798–806, doi: [10.2174/1573405613666170428160219](https://doi.org/10.2174/1573405613666170428160219).
20. Ozer E, Icke C, Arda N. Microanatomical study of the intracranial abducens nerve: clinical interest and surgical perspective. *Turk Neurosurg.* 2010; 20(4): 449–456, doi: [10.5137/1019-5149.JTN.3303-10.1](https://doi.org/10.5137/1019-5149.JTN.3303-10.1), indexed in Pubmed: [20963693](https://pubmed.ncbi.nlm.nih.gov/20963693/).
21. Özgür A, Esen K. Ossification of the petrosphenoidal ligament: multidetector computed tomography findings of an unusual variation with a potential role in abducens nerve palsy. *Jpn J Radiol.* 2015; 33(5): 260–265, doi: [10.1007/s11604-015-0410-9](https://doi.org/10.1007/s11604-015-0410-9), indexed in Pubmed: [25749833](https://pubmed.ncbi.nlm.nih.gov/25749833/).
22. Ozveren MF, Sam B, Akdemir I, et al. Duplication of the abducens nerve at the petroclival region: an anatomic study. *Neurosurgery.* 2003; 52(3): 645–652, doi: [10.1227/01.neu.0000048186.18741.3c](https://doi.org/10.1227/01.neu.0000048186.18741.3c), indexed in Pubmed: [12590690](https://pubmed.ncbi.nlm.nih.gov/12590690/).
23. Rzymyski K, Kosowicz J. The skull in gonadal dysgenesis. A roentgenometric study. *Clin Radiol.* 1975; 26(3): 379–384, doi: [10.1016/s0009-9260\(75\)80082-1](https://doi.org/10.1016/s0009-9260(75)80082-1), indexed in Pubmed: [1201635](https://pubmed.ncbi.nlm.nih.gov/1201635/).
24. Sedghizadeh PP, Nguyen M, Enciso R. Intracranial physiological calcifications evaluated with cone beam CT. *Dentomaxillofac Radiol.* 2012; 41(8): 675–678, doi: [10.1259/dmfr/33077422](https://doi.org/10.1259/dmfr/33077422), indexed in Pubmed: [22842632](https://pubmed.ncbi.nlm.nih.gov/22842632/).
25. Skrzat J, Walocha J, Jaworek JK, et al. The clinical significance of the petroclinoid ligament. *Folia Morphol.* 2007; 66(1): 39–43, indexed in Pubmed: [17533593](https://pubmed.ncbi.nlm.nih.gov/17533593/).
26. Stanton JB, Wilkinson M. Familial calcification of the petrosphenoidal ligament. *Lancet.* 1949; 2(6582): 736–737, doi: [10.1016/s0140-6736\(49\)92258-8](https://doi.org/10.1016/s0140-6736(49)92258-8), indexed in Pubmed: [15390690](https://pubmed.ncbi.nlm.nih.gov/15390690/).
27. Tomio R, Toda M, Sutiono AB, et al. Grüber's ligament as a useful landmark for the abducens nerve in the transnasal approach. *J Neurosurg.* 2015; 122(3): 499–503, doi: [10.3171/2014.10.JNS132437](https://doi.org/10.3171/2014.10.JNS132437), indexed in Pubmed: [25380109](https://pubmed.ncbi.nlm.nih.gov/25380109/).
28. Touska P, Hasso S, Oztek A, et al. Skull base ligamentous mineralisation: evaluation using computed tomography and a review of the clinical relevance. *Insights Imaging.* 2019; 10(1): 55, doi: [10.1186/s13244-019-0740-8](https://doi.org/10.1186/s13244-019-0740-8), indexed in Pubmed: [31115710](https://pubmed.ncbi.nlm.nih.gov/31115710/).
29. Tsitsopoulos PD, Tsonidis CA, Petsas GP, et al. Microsurgical study of the Dorello's canal. *Skull Base Surg.* 1996; 6(3): 181–185, doi: [10.1055/s-2008-1058643](https://doi.org/10.1055/s-2008-1058643), indexed in Pubmed: [17170976](https://pubmed.ncbi.nlm.nih.gov/17170976/).
30. Tubbs RS, Radcliff V, Shoja MM, et al. Dorello canal revisited: an observation that potentially explains the frequency of abducens nerve injury after head injury. *World Neurosurg.* 2012; 77(1): 119–121, doi: [10.1016/j.wneu.2011.03.046](https://doi.org/10.1016/j.wneu.2011.03.046), indexed in Pubmed: [22130113](https://pubmed.ncbi.nlm.nih.gov/22130113/).
31. Tubbs RS, Sharma A, Loukas M, et al. Ossification of the petrosphenoidal ligament: unusual variation with the potential for abducens nerve entrapment in Dorello's canal at the skull base. *Surg Radiol Anat.* 2014; 36(3): 303–305, doi: [10.1007/s00276-013-1171-8](https://doi.org/10.1007/s00276-013-1171-8), indexed in Pubmed: [23877841](https://pubmed.ncbi.nlm.nih.gov/23877841/).
32. Umansky F, Elidan J, Valarezo A. Dorello's canal: a microanatomical study. *J Neurosurg.* 1991; 75(2): 294–298, doi: [10.3171/jns.1991.75.2.0294](https://doi.org/10.3171/jns.1991.75.2.0294), indexed in Pubmed: [2072168](https://pubmed.ncbi.nlm.nih.gov/2072168/).
33. Wysiadecki G, Orkisz S, Gałązkiewicz-Stolarczyk M, et al. The abducens nerve: its topography and anatomical variations in intracranial course with clinical commentary. *Folia Morphol.* 2015; 74(2): 236–244, doi: [10.5603/FM.2015.0037](https://doi.org/10.5603/FM.2015.0037), indexed in Pubmed: [26050813](https://pubmed.ncbi.nlm.nih.gov/26050813/).
34. Wysiadecki G, Radek M, Tubbs RS, et al. Microsurgical anatomy of the inferomedial paraclival triangle: contents, topographical relationships and anatomical variations. *Brain Sci.* 2021; 11(5): 596, doi: [10.3390/brainsci11050596](https://doi.org/10.3390/brainsci11050596), indexed in Pubmed: [34064376](https://pubmed.ncbi.nlm.nih.gov/34064376/).
35. Żytkowski A, Clarke E, Musiał A, et al. Atypical attachment of the petrosphenoidal (petroclival) ligament to the posterior genu of the cavernous internal carotid artery: case report. *Transl Res Anat.* 2022; 27: 100185, doi: [10.1016/j.tria.2022.100185](https://doi.org/10.1016/j.tria.2022.100185).